

Theoretical Insight into the Mechanism of [3 + 2] Cycloaddition Reactions of 1,3-Disila-2-group-13 Atomic Anions [$>Si=M=Si<$][−] (M = B, Al, Ga, In, and Tl)

Jun Hsiao and Ming-Der Su*

Department of Applied Chemistry, National Chiayi University, Chiayi 60004, Taiwan, Republic of China

Received March 27, 2007

The potential energy surfaces for the cycloaddition reactions of 12-valence-electron allenic anion species have been studied using density functional theory (B3LYP/LANL2DZ). Five allenic anions of the form $[(SiH_3)_2Si=M=Si(SiH_3)_2]^-$, where M = B, Al, Ga, In, and Tl, have been chosen as model reactants in this work. Also, the alkene cycloaddition has been used to study the chemical reactivities of these 12-valence-electron allenic anions. The present theoretical investigations suggest that the reactivity of 12-valence-electron allenic anions increases in the order $B \ll Al \approx Ga \approx In < Tl$. That is, a less electronegative as well as a heavier main group atom center M will facilitate the cycloaddition reaction. Furthermore, the singlet–triplet energy splitting of the 12-valence-electron allenic anions, as described in the configuration mixing model attributed to the work of Pross and Shaik, can be used as a diagnostic tool to predict their reactivities. The results obtained allow a number of predictions to be made.

1. Introduction

There has been considerable research interest over the last two decades concentrating on the chemistry of multiple-bond systems, involving heavier main group elements with low coordination number.¹ Most have been isolated as stable compounds by taking advantage of kinetic stabilization by using appropriately bulky substituents as steric protection groups. Among the many stable multiple-bond systems that have been successfully characterized, compounds with π -bonds to group 14 as well as group 15 elements were the first stable examples to be synthesized² and still play an important role in this field.³ In contrast, the number of analogous compounds involving

double bonds to the heavier group 13 elements has remained quite small.⁴ Of these, the syntheses of stable double-bond compounds between silicon and group 13 elements have been a particular challenge to synthetic chemists.

Through the elegant studies performed by Sekiguchi and many co-workers, kinetically stabilized molecules having the $>Si=Ga=Si<$ or $>Si=In=Si<$ units, representing novel allenic anionic species of the main group elements, have been synthesized and fully characterized.⁵ One of these is the 1,1,3,3-tetrakis(di-*tert*-butylmethylsilyl)-1,3-disila-2-gallataallenic anion, $[(t-Bu_2MeSi)_2Si=Ga=Si(t-Bu_2MeSi)_2]^-$, a novel multiply bonded system involving silicon and gallium. The other is the first stable 1,1,3,3-tetrakis(di-*tert*-butylmethylsilyl)-1,3-disila-2-indataallenic anion, $[(t-Bu_2MeSi)_2Si=In=Si(t-Bu_2MeSi)_2]^-$, which has been isolated, again by taking advantage of bulky substituent groups. As a result, doubly bonded systems between heavier group 13 and group 14 elements are no longer imaginary species. Nevertheless, attempts to isolate other analogues, such as $[(t-Bu_2MeSi)_2Si=B=Si(t-Bu_2MeSi)_2]^-$ and $[(t-Bu_2MeSi)_2Si=Tl=Si(t-Bu_2MeSi)_2]^-$, have all been unsuccessful up to now.

The purpose of the present work is therefore to enlarge the previous experimental approaches by studying the reactivity of $Si=M$ doubly bonded systems, with M varying from boron to thallium. Our object is to obtain more insight into the bonding character of their various isomers and to provide theoretical information on the thermodynamic and kinetic stability of the various $>Si=M=Si<$ (M = group 13 elements) species. To achieve this, it is necessary to determine the transition-state (TS) geometries of the molecules as well as the ground-state energies of the products. To the best of our knowledge, neither

* To whom correspondence should be addressed. E-mail: midesu@mail.nyu.edu.tw.

(1) For recent reviews, see: (a) Cowley, A. H. *Polyhedron* **1984**, *3*, 389. (b) Cowley, A. H. *Acc. Chem. Res.* **1984**, *17*, 386. (c) Cowley, A. H.; Norman, N. C. *Prog. Inorg. Chem.* **1986**, *34*, 1. (d) Scherer, O. J. *Angew. Chem., Int. Ed. Engl.* **1990**, *29*, 1104. (e) Weber, L. *Chem. Rev.* **1992**, *92*, 1839. (f) Escudie, J.; Couret, C.; Ranaivonjatovo, H.; Satge, J. *Coord. Chem. Rev.* **1994**, *130*, 427. (g) Driess, M. *Coord. Chem. Rev.* **1995**, *145*, 1. (h) Okazaki, R.; West, R. *Adv. Organomet. Chem.* **1996**, *39*, 31. (i) Klinkhammer, K. W. *Angew. Chem., Int. Ed. Engl.* **1997**, *36*, 2320. (j) Barrau, J.; Rina, G. *Coord. Chem. Rev.* **1998**, *178*, 593. (k) Power, P. P. *J. Chem. Soc., Dalton Trans.* **1998**, 2939. (l) Tokitoh, N.; Matsumoto, T.; Okazaki, R. *Bull. Chem. Soc. Jpn.* **1999**, *72*, 1665. (m) Robinson, G. H. *Acc. Chem. Res.* **1999**, *32*, 773. (n) Leigh, W. J. *Pure Appl. Chem.* **1999**, *71*, 453. (o) Tokitoh, N. *Pure Appl. Chem.* **1999**, *71*, 495. (p) Power, P. P. *Chem. Rev.* **1999**, *99*, 3463. (q) Jones, C. *Coord. Chem. Rev.* **2001**, *215*, 151. (r) Grutzmacher, H.; Fassler, T. F. *Chem.–Eur. J.* **2000**, *6*, 2317. (s) Clyburne, J. A. C.; McMullen, N. *Coord. Chem. Rev.* **2000**, *210*, 73. (t) Sasamori, T.; Arai, Y.; Takeda, N.; Okazaki, R.; Furukawa, Y.; Kimura, M.; Nagase, S.; Tokitoh, N. *Bull. Chem. Soc. Jpn.* **2002**, *75*, 661.

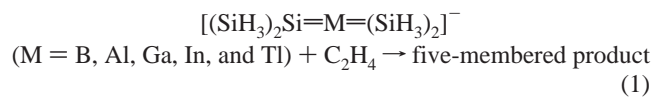
(2) (a) Brook, A. G.; Abdesaken, F.; Gutekunst, B.; Gutekunst, G.; Kallury, R. K. *J. Chem. Soc., Chem. Commun.* **1981**, 191. (b) West, R.; Fink, M. J.; Michl, J. *Science* **1981**, *214*, 1343. (c) Smit, C. N.; Lock, F. M.; Bickelhaupt, F. *Tetrahedron Lett.* **1984**, *25*, 3011. (d) Wiberg, N.; Schurz, K.; Fisher, G. *Angew. Chem., Int. Ed. Engl.* **1985**, *24*, 1053. (e) Wiberg, N.; Schurz, K.; Reber, G.; Müller, G. *J. Chem. Soc., Chem. Commun.* **1986**, 591. (f) Smit, C. N.; Bickelhaupt, F. *Organometallics* **1987**, *6*, 1156. (g) Niesmann, J.; Klingebiel, U.; Schäfer, M.; Boese, R. *Organometallics* **1998**, *17*, 947. (h) Driess, M.; Rell, S.; Pritzkow, H. *J. Chem. Soc., Chem. Commun.* **1995**, 253. (i) Suzuki, H.; Tokitoh, N.; Nagase, S.; Okazaki, R. *J. Am. Chem. Soc.* **1994**, *116*, 11578. (j) Suzuki, H.; Tokitoh, N.; Okazaki, R.; Nagase, S.; Goto, M. *J. Am. Chem. Soc.* **1998**, *120*, 11096.

(3) (a) Weidenbruch, M. *Eur. J. Inorg. Chem.* **1999**, 373. (b) Power, P. P. *Chem. Rev.* **1999**, *99*, 3463. (c) Escudie, J.; Ranaivonjatovo, H. *Adv. Organomet. Chem.* **1999**, *44*, 113. (d) Weidenbruch, M. *Organometallics* **2003**, *22*, 4348. (e) Escudie, J.; Ranaivonjatovo, H.; Rigon, L. *Chem. Rev.* **2000**, *100*, 3639. (f) Eichler, B.; West, R. *Adv. Organomet. Chem.* **2000**, *46*, 1. (g) Ishida, S.; Iwamoto, T.; Kabuto, C.; Kira, M. *Nature* **2003**, *421*, 725.

(4) Nakata, N.; Sekiguchi, A. *J. Am. Chem. Soc.* **2006**, *128*, 422.

(5) Nakata, N.; Izumi, R.; Lee, V. Y.; Ichinohe, M.; Sekiguchi, A. *J. Am. Chem. Soc.* **2004**, *126*, 5058.

experimental nor theoretical studies have yet been performed on allenic anions with main group elements, let alone a systematic theoretical study of elemental effects on the reactivities of such species. This aroused our interest to investigate the potential energy surfaces of $[>\text{Si}=\text{M}=\text{Si}<]^-$ reactions using density functional theory (DFT). A study of the important [3 + 2] cycloaddition reaction, eq 1, was thus undertaken.



For the present, our focus is on the cycloaddition reaction of allenic anions of the form $[(\text{SiH}_3)_2\text{Si}=\text{M}=\text{Si}(\text{SiH}_3)_2]^-$, where $\text{M} = \text{B}, \text{Al}, \text{Ga}, \text{In}, \text{and Tl}$. These compounds are all isoelectronic and contain 12 valence electrons.⁶

The reason for choosing eq 1 as the model is simply because we acknowledge that the size of the experimental systems prevents highly accurate optimizations in our quantum theoretical calculations. In particular, the cost and available computational facilities make them impractical. As a consequence, we have chosen small substituent groups for the allenic fragments. Through this theoretical study, we hope (a) to obtain a detailed understanding of the [3 + 2] cycloaddition reactions of ethylene with $[(\text{SiH}_3)_2\text{Si}=\text{M}=\text{Si}(\text{SiH}_3)_2]^-$ -type complexes, (b) to investigate the influence of different group 13 atomic centers on the geometries and energies of the transition states, (c) to elucidate the differences between these group 13 elements, (d) to probe electronic effects on the reactivities, and (e) to reveal factors that control the activation barriers for such cycloaddition reactions. It is our intention to show clearly that the singlet–triplet gap in the $[(\text{SiH}_3)_2\text{Si}=\text{M}=\text{Si}(\text{SiH}_3)_2]^-$ species can be used as a diagnostic tool to predict its reactivity toward cycloaddition reactions. In particular, the predicted molecular parameters presented in this paper will act as a guide for any future experimental investigations on some unknown $[>\text{Si}=\text{M}=\text{Si}<]^-$ ($\text{M} = \text{group 13 elements}$) isomers.

II. Methodology

All geometries were fully optimized without imposing any symmetry constraints, although in some instances the resulting structures showed various elements of symmetry. For our DFT calculations, we used the hybrid gradient-corrected exchange functional proposed by Becke,⁷ combined with the gradient-corrected correlation functional of Lee, Yang, and Parr.⁸ This functional is commonly known as B3LYP and has been shown to be quite reliable for both geometries and energies.⁹ These B3LYP calculations were carried out with relativistic effective core potentials on the group 13 elements modeled using the double- ζ (DZ) basis sets¹⁰ augmented by a set of d-type polarization

(6) According to a reviewer's comment, multiply bonded compounds of heavier main group elements often undergo [2 + 2] reactions with alkenes and alkynes. In fact, we have checked the [2 + 2] reactions using the RHF/3-21G(d), B3LYP/3-21G(d), RHF/LANL2DZ, and B3LYP/6-31G(d) levels of theory. However, they all failed. Only the [3 + 2] reactions can work based on the present theoretical calculations.

(7) (a) Becke, A. D. *Phys. Rev. A* **1988**, *38*, 3098. (b) Becke, A. D. *J. Chem. Phys.* **1993**, *98*, 5648.

(8) Lee, C.; Yang, W.; Parr, R. G. *Phys. Rev. B* **1988**, *37*, 785.

(9) (a) Su, M.-D. *J. Phys. Chem. A* **2004**, *108*, 823. (b) Su, M.-D. *Inorg. Chem.* **2004**, *43*, 4846. (c) Su, M.-D. *Eur. J. Chem.* **2004**, *10*, 5877, and related references therein.

(10) (a) Dunning, T. H., Jr.; Hay, P. J. In *Modern Theoretical Chemistry*; Schaefer, H. F., III, Ed.; Plenum: New York, 1976; pp 1–28. (b) Hay, P. J.; Wadt, W. R. *J. Chem. Phys.* **1985**, *82*, 270. (c) Hay, P. J.; Wadt, W. R. *J. Chem. Phys.* **1985**, *82*, 284. (d) Hay, P. J.; Wadt, W. R. *J. Chem. Phys.* **1985**, *82*, 299. (e) Check, C. E.; Faust, T. O.; Bailey, J. M.; Wright, B. J.; Gilbert, T. M.; Sunderlin, L. S. *J. Phys. Chem. A* **2001**, *105*, 8111.

functions.^{10e} The DZ basis set for the hydrogen element was augmented by a set of p-type polarization functions (p exponents 0.356). Accordingly, we denote our B3LYP calculations by B3LYP/LANL2DZ.¹¹ The spin-unrestricted (UB3LYP) formalism was used for the open-shell (triplet) species. The computed expectation values of the spin-squared operator $\langle S^2 \rangle$ were in the range 2.001–2.007 for all the triplet species considered here. They were therefore very close to the correct value of 2.0 for pure triplets, so that the resultant geometries and energetics are reliable for this study. Frequency calculations were performed on all structures to confirm that the reactants and products had no imaginary frequencies and that transition states possessed a single imaginary frequency. The relative energies were thus corrected for vibrational zero-point energies (ZPE, not scaled).

For better energetics, single-point energies were also calculated at CCSD(FC)/LANL2DZ//B3LYP/LANL2DZ + ZPE (B3LYP/LANL2DZ) (hereafter designed CCSD),¹¹ to improve the treatment of electron correlation. All of the theoretical calculations were performed using the GAUSSIAN 03 package of programs.¹³

III. Results and Discussion

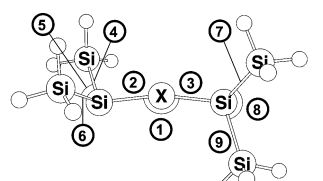
(1) Geometries and Electronic Structures of $[(\text{SiH}_3)_2\text{Si}=\text{M}=\text{Si}(\text{SiH}_3)_2]^-$. Before discussing the geometrical optimizations and the potential energy surfaces for the chemical reactions of the 12-valence-electron allenic anions, we shall first examine the geometries and electronic structures of the reactants, i.e., $[(\text{SiH}_3)_2\text{Si}=\text{M}=\text{Si}(\text{SiH}_3)_2]^-$ ($\text{M} = \text{B}, \text{Al}, \text{Ga}, \text{In}, \text{and Tl}$). The optimized geometries for these 12-valence-electron allenic anions were calculated at the B3LYP/LANL2DZ level of theory, and their selected geometrical parameters are collected in Figures 1 and 2, where they are compared with some available experimental data.⁵ The relative energies obtained by B3LYP and CCSD calculations are summarized in Table 1. Their Cartesian coordinates are included in the Supporting Information.

In the present work, reactants $[(\text{SiH}_3)_2\text{Si}=\text{M}=\text{Si}(\text{SiH}_3)_2]^-$ ($\text{M} = \text{B}, \text{Al}, \text{Ga}, \text{In}, \text{and Tl}$) have been calculated both as singlet and as triplet species, whose geometric parameters are shown in Figures 1 and 2, respectively. The theoretical findings based on the B3LYP and CCSD calculations indicate that all the anions possess a singlet ground state. As mentioned earlier, although only two crystallographic investigations on substituted $[>\text{Si}=\text{Ga}=\text{Si}<]^-$ and $[>\text{Si}=\text{In}=\text{Si}<]^-$ have been carried out during the last three years, no theoretical calculations are so far available in the literature for these compounds. Our B3LYP

(11) It was reported that the shape and symmetry properties of the Kohn–Sham orbitals are very similar to those calculated by the Hartree–Fock method. The energy order of the occupied orbitals is in most cases in agreement among the various methods. We are thus confident that the present calculation results should be reliable. See: Stowasser, R.; Hoffmann, R. *J. Am. Chem. Soc.* **1999**, *121*, 3414.

(12) Pople, J. A.; Head-Gordon, M.; Raghavachari, K. *J. Chem. Phys.* **1987**, *87*, 5968.

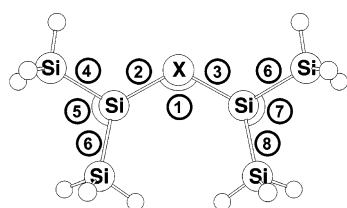
(13) Frisch, M. J.; Trucks, G. W.; Schlegel, H. B.; Scuseria, G. E.; Robb, M. A.; Cheeseman, J. R.; Zakrzewski, V. G.; Montgomery, J. A., Jr.; Vreven, T.; Kudin, K. N.; Burant, J. C.; Millam, J. M.; Iyengar, S. S.; Tomasi, J.; Barone, V.; Mennucci, B.; Cossi, M.; Scalmani, G.; Rega, N.; Petersson, G. A.; Nakatsuji, H.; Hada, M.; Ehara, M.; Toyota, K.; Fukuda, R.; Hasegawa, J.; Ishida, M.; Nakajima, T.; Honda, Y.; Kitao, O.; Nakai, H.; Klene, M.; Li, X.; Knox, J. E.; Hratchian, H. P.; Cross, J. B.; Adamo, C.; Jaramillo, J.; Gomperts, R.; Stratmann, R. E.; Yazyev, O.; Austin, A. J.; Cammi, R.; Pomelli, C.; Ochterski, J. W.; Ayala, P. Y.; Morokuma, K.; Voth, G. A.; Salvador, P.; Dannenberg, J. J.; Zakrzewski, V. G.; Dapprich, S.; Daniels, A. D.; Strain, M. C.; Farkas, O.; Malick, D. K.; Rabuck, A. D.; Raghavachari, K.; Foresman, J. B.; Ortiz, J. V.; Cui, Q.; Baboul, A. G.; Clifford, S.; Cioslowski, J.; Stefanov, B. B.; Liu, G.; Liashenko, A.; Piskorz, P.; Komaromi, I.; Martin, R. L.; Fox, D. J.; Keith, T.; Al-Laham, M. A.; Peng, C. Y.; Nanayakkara, A.; Challacombe, M.; Gill, P. M. W.; Johnson, B.; Chen, W.; Wong, M. W.; Gonzalez, C.; Pople, J. A. *GAUSSIAN 03*; Gaussian, Inc., Wallingford, CT, 2003.



**Reactant
(Singlet)**

X	B	Al	Ga	In	Tl
①	170.2	153.7	155.0 (161.6)	154.4 (161.3)	154.8
②	1.858	2.371	2.360 (2.277)	2.542 (2.479)	2.708
③	1.858	2.369	2.360 (2.282)	2.543 (2.484)	2.708
④	2.330	2.366	2.372 (2.361)	2.381 (2.376)	2.399
⑤	114.0	106.6	105.5 (117.0)	104.1 (107.9)	102.0
⑥	2.331	2.367	2.373 (2.356)	2.384 (2.325)	2.403
⑦	2.330	2.364	2.372 (2.362)	2.382 (2.366)	2.399
⑧	114.1	106.3	105.5 (118.1)	104.2 (110.1)	101.9
⑨	2.331	2.368	2.373 (2.362)	2.385 (2.380)	2.404

Figure 1. B3LYP/LANL2DZ-optimized geometries (in Å and deg) of the reactants (singlet) $[(\text{SiH}_3)_2\text{Si}=\text{M}=\text{Si}(\text{SiH}_3)_2]^-$ (X = B, Al, Ga, In, and Tl). The experimental values (see ref 4) are in parentheses. For the relative energies for each species see Table 1. Hydrogens are omitted for clarity.



**Reactant
(Triplet)**

X	B	Al	Ga	In	Tl
①	157.5	120.0	117.7	108.5	101.9
②	1.884	2.429	2.444	2.693	3.039
③	1.884	2.430	2.444	2.688	3.038
④	2.344	2.356	2.365	2.376	2.387
⑤	110.3	106.6	105.3	103.5	102.2
⑥	2.355	2.359	2.367	2.376	2.383
⑦	2.344	2.357	2.365	2.377	2.389
⑧	110.3	106.5	105.4	103.4	102.2
⑨	2.355	2.360	2.367	2.377	2.381

Figure 2. B3LYP/LANL2DZ-optimized geometries (in Å and deg) of the reactants (triplet) $[(\text{SiH}_3)_2\text{Si}=\text{M}=\text{Si}(\text{SiH}_3)_2]^-$ (X = B, Al, Ga, In, and Tl). For the relative energies for each species see Table 1. Hydrogens are omitted for clarity.

calculations predict that the average Si=Ga and Si=In bond lengths in the singlet state are 2.360 and 2.542 Å, which are consistent with the experimental values (2.280 and 2.482 Å), respectively. Similarly, the calculated Si–Si bond lengths in $[(\text{SiH}_3)_2\text{Si}=\text{Ga}=\text{Si}(\text{SiH}_3)_2]^-$ (average 2.372 Å at B3LYP) and $[(\text{SiH}_3)_2\text{Si}=\text{In}=\text{Si}(\text{SiH}_3)_2]^-$ (average 2.382 Å at B3LYP) compare favorably with average Si–Si bond lengths determined from X-ray data in $[>\text{Si}=\text{Ga}=\text{Si}<]^-$ (2.361 Å) and $[>\text{Si}=\text{In}=\text{Si}<]^-$ (2.362 Å), respectively, reported by Sekiguchi et al.⁵ On the other hand, the SiGaSi angle in $[(\text{SiH}_3)_2\text{Si}=\text{Ga}=\text{Si}(\text{SiH}_3)_2]^-$ and SiInSi angle in $[(\text{SiH}_3)_2\text{Si}=\text{In}=\text{Si}(\text{SiH}_3)_2]^-$ are 155.0° and 154.4°, which are in reasonable agreement with the experimental values (161.6° and 161.4°, respectively) as given in Figure 1, bearing in mind that the experimental

Table 1. Relative Energies for Singlet and Triplet Cycloaddition Process: Reactants $[(\text{SiH}_3)_2\text{Si}=\text{M}=\text{Si}(\text{SiH}_3)_2]^- + \text{C}_2\text{H}_4 \rightarrow$ Transition State \rightarrow Cycloaddition Product^a

system	ΔE_{st}^b (kcal mol ⁻¹)	ΔE^\ddagger^c (kcal mol ⁻¹)	ΔH^\ddagger^d (kcal mol ⁻¹)
M = B	82.76 (88.18)	36.03 (38.30)	11.28 (5.289)
M = Al	75.75 (77.94)	16.14 (12.90)	-30.19 (-39.13)
M = Ga	77.81 (80.44)	18.28 (14.88)	-30.66 (-39.23)
M = In	74.19 (76.34)	16.11 (12.20)	-37.06 (-47.07)
M = Tl	66.00 (72.68)	14.46 (11.81)	-45.66 (-51.82)

^a Energy differences have been zero-point corrected. See the text. All were calculated at the B3LYP/LANL2DZ (CCSD results in parentheses) level of theory. For the B3LYP-optimized structures of the stationary points see Figures 1, 2, 4, and 5. ^b Energy relative to the corresponding singlet state. A positive value means the singlet is the ground state. ^c The activation energy of the transition state, relative to the corresponding reactants. ^d The reaction enthalpy of the product, relative to the corresponding reactants.

structures contain bulkier groups. Namely, the discrepancy may be attributed to steric effects that cause substituted $[>\text{Si}=\text{Ga}=\text{Si}<]^-$ and $[>\text{Si}=\text{In}=\text{Si}<]^-$ to have larger Si=M=Si bond angles than in $[(\text{SiH}_3)_2\text{Si}=\text{Ga}=\text{Si}(\text{SiH}_3)_2]^-$ and $[(\text{SiH}_3)_2\text{Si}=\text{In}=\text{Si}(\text{SiH}_3)_2]^-$, respectively. In any event, due to the agreement between the B3LYP theory and the available experimental data, one would therefore expect that the same relative accuracy should also apply to the geometries and to the energetics predicted for the other $[(\text{SiH}_3)_2\text{Si}=\text{M}=\text{Si}(\text{SiH}_3)_2]^-$ (M = group 13 elements) species.

In order to gain more insight into the nature of the chemical bonding in the series of $[(\text{SiH}_3)_2\text{Si}=\text{M}=\text{Si}(\text{SiH}_3)_2]^-$ anions, the valence molecular orbitals based on the B3LYP/LANL2DZ calculations are represented in Figure 3. Basically, all the group 13 allenic anion species ($[>\text{Si}=\text{M}=\text{Si}<]^-$) have in common a four atomic orbital π -system containing four π -electrons analogous to an allene species (a-b-c),¹⁴ which can interact with an olefin in a six-electron transition state, energetically favored according to the Woodward–Hoffmann rules.¹⁵ It is apparent from Figure 3 that in the triplet state one electron is situated in the LUMO, in which antibonding interactions exist between the center and the terminal atoms. On the other hand, a bonding interaction exists between the center and the terminal atoms in the HOMO. The bond distances $r(\text{a}-\text{b})$ and $r(\text{c}-\text{b})$ are therefore expected to be longer, and the bond angle $\angle \text{a}-\text{b}-\text{c}$ is expected to be smaller for the triplet compared to the singlet. These predictions agree qualitatively with our B3LYP/LANL2DZ results for all cases as given in Figures 1 and 2. For instance, our B3LYP computations demonstrate that singlet $[(\text{SiH}_3)_2\text{Si}=\text{B}=\text{Si}(\text{SiH}_3)_2]^-$ (170°) > triplet $[(\text{SiH}_3)_2\text{Si}=\text{B}=\text{Si}(\text{SiH}_3)_2]^-$ (156°), singlet $[(\text{SiH}_3)_2\text{Si}=\text{Al}=\text{Si}(\text{SiH}_3)_2]^-$ (154°) > triplet $[(\text{SiH}_3)_2\text{Si}=\text{Al}=\text{Si}(\text{SiH}_3)_2]^-$ (120°), singlet $[(\text{SiH}_3)_2\text{Si}=\text{Ga}=\text{Si}(\text{SiH}_3)_2]^-$ (155°) > triplet $[(\text{SiH}_3)_2\text{Si}=\text{Ga}=\text{Si}(\text{SiH}_3)_2]^-$ (118°), singlet $[(\text{SiH}_3)_2\text{Si}=\text{In}=\text{Si}(\text{SiH}_3)_2]^-$ (154°) > triplet $[(\text{SiH}_3)_2\text{Si}=\text{In}=\text{Si}(\text{SiH}_3)_2]^-$ (109°), and singlet $[(\text{SiH}_3)_2\text{Si}=\text{Tl}=\text{Si}(\text{SiH}_3)_2]^-$ (155°) > triplet $[(\text{SiH}_3)_2\text{Si}=\text{Tl}=\text{Si}(\text{SiH}_3)_2]^-$ (102°). It should be noted that the triplet $\angle \text{SiMSi}$ bond angles at the group 13 elemental centers in $[(\text{SiH}_3)_2\text{Si}=\text{Al}=\text{Si}(\text{SiH}_3)_2]^-$, $[(\text{SiH}_3)_2\text{Si}=\text{Ga}=\text{Si}(\text{SiH}_3)_2]^-$, $[(\text{SiH}_3)_2\text{Si}=\text{In}=\text{Si}(\text{SiH}_3)_2]^-$, and $[(\text{SiH}_3)_2\text{Si}=\text{Tl}=\text{Si}(\text{SiH}_3)_2]^-$,

(14) Jorgenson, W. L.; Salem, L. In *The Organic Chemist's Book of Orbitals*; Academic Press: New York, 1973; pp 122–125.

(15) (a) Woodward, R. B.; Hoffmann, R. *Angew. Chem., Int. Ed. Engl.* **1969**, *8*, 781. (b) Woodward, R. B.; Hoffmann, R. *Angew. Chem., Int. Ed. Engl.* **1969**, *8*, 817.

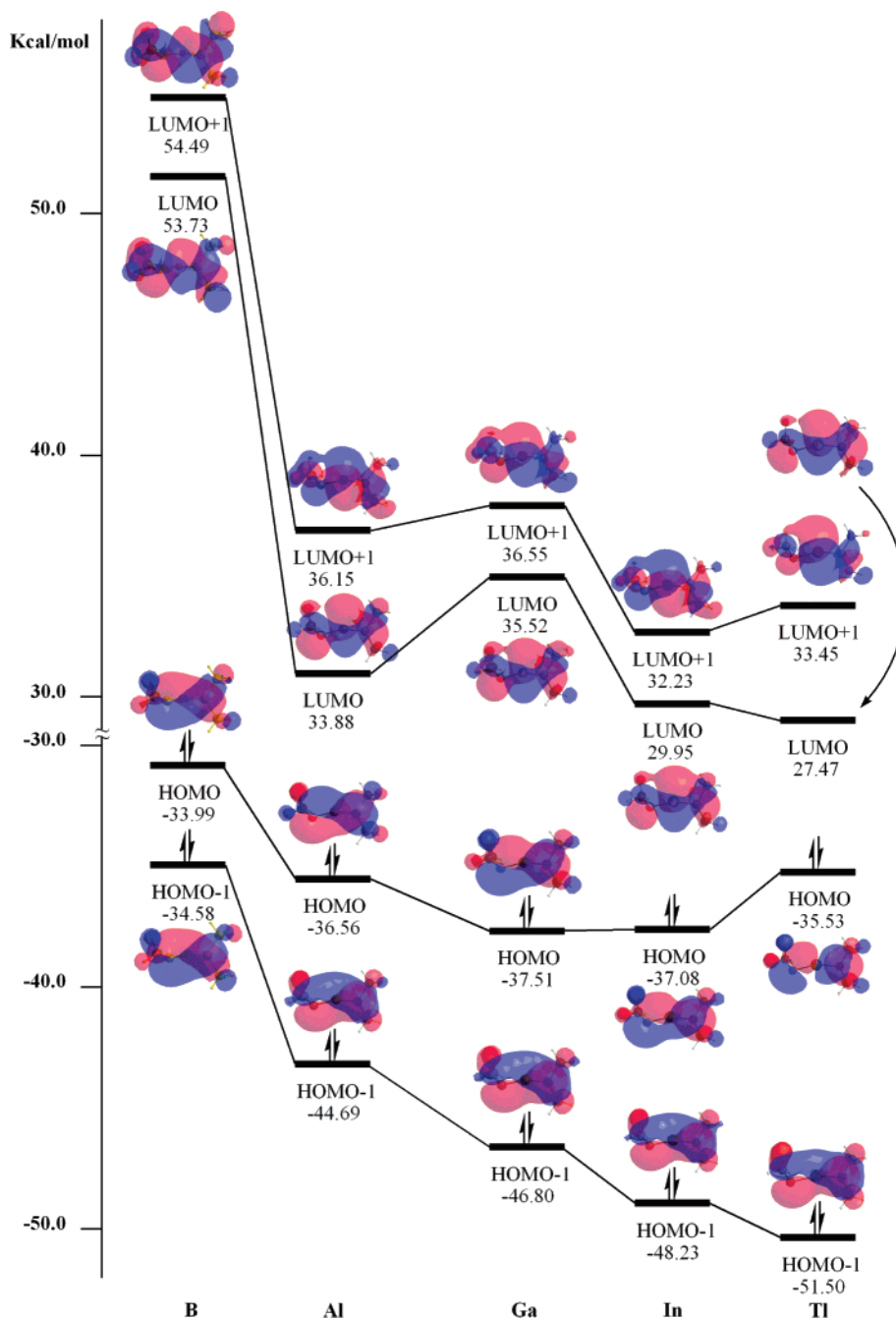


Figure 3. Calculated frontier molecular orbital for the $[(\text{SiH}_3)_2\text{Si}=\text{M}=\text{Si}(\text{SiH}_3)_2]^-$ ($\text{X} = \text{B}, \text{Al}, \text{Ga}, \text{In}, \text{and Tl}$) species. For more information see the text.

respectively, decrease, as expected, in the given order 156° (B) $> 120^\circ$ (Al) $> 118^\circ$ (Ga) $> 109^\circ$ (In) $> 102^\circ$ (Tl). However, the singlet $\angle\text{SiMSi}$ bond angles follow a different trend: 170° (B) $> 155^\circ$ (Ga) $\approx 155^\circ$ (Tl) $> 154^\circ$ (In) $\approx 154^\circ$ (Al).

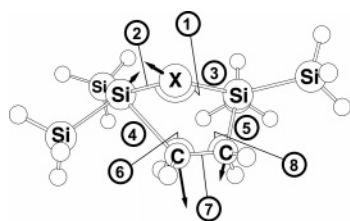
Furthermore, the most striking results are the singlet–triplet energy separations of the 12-valence-electron allenic anions. It is often observed¹⁶ that the singlet–triplet energy splitting in analogous species increases with the atomic number of the central atom. However, in the case of group 13 allenic anions, the singlet–triplet energy splitting follows a somewhat different trend. For example, our theoretical results as given in Table 1 indicate an intriguing trend, $+88$ kcal/mol (B) $> +80$ kcal/mol (Ga) $> +78$ kcal/mol (Al) $> +76$ kcal/mol (In) $> +72$

kcal/mol (Tl) at the CCSD level of theory. As there are no relevant experimental and theoretical data on such quantities, the above result is a prediction. We shall use the above results to explain the origin of barrier heights for the [3 + 2] cycloaddition reactions in a later section.

In addition, according to Su's work¹⁷ based on perturbation theory, it is predicted that for 12-valence-electron three-center systems, substitution of more electronegative atoms is most energetically favorable at the terminal positions. Indeed, examining the electronegativities of silicon, gallium, and indium, it is found that the electronegativity of Si (1.7) is greater than that of both Ga (1.6) and In (1.5).¹⁵ This suggests that in the $[>\text{Si}=\text{Ga}=\text{Si}<]^-$ and $[>\text{Si}=\text{In}=\text{Si}<]^-$ π -systems, the less electronegative atom (such as Ga and In) will occur preferably

(16) (a) Su, M.-D. *J. Phys. Chem. A* **2002**, *106*, 9563. (b) Su, M.-D. *Eur. J. Chem.* **2004**, *10*, 5877.

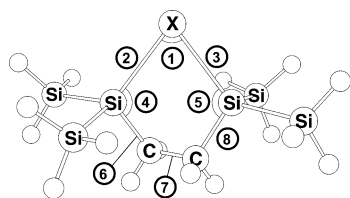
(17) Su, M. D. *Int. J. Quantum Chem.* **1993**, *48*, 249.



Transition state

X	B	Al	Ga	In	Tl
①	129.4	96.00	95.23	92.67	94.79
②	1.854	2.433	2.438	2.620	2.831
③	1.957	2.605	2.618	2.797	3.001
④	2.330	2.806	2.890	3.076	3.556
⑤	1.939	1.968	1.968	1.975	1.988
⑥	113.8	121.0	119.3	119.2	119.1
⑦	1.559	1.552	1.546	1.539	1.517
⑧	105.1	109.8	110.0	112.1	114.6

Figure 4. B3LYP/LANL2DZ-optimized geometries (in Å and deg) of the transition states of $[(\text{SiH}_3)_2\text{Si}=\text{M}=\text{Si}(\text{SiH}_3)_2]^-$ (X = B, Al, Ga, In, and Tl) and ethylene molecules. For the relative energies for each species see Table 1. The heavy arrows indicate the main atomic motions in the transition-state eigenvector. Hydrogens are omitted for clarity.



Product

X	B	Al	Ga	In	Tl
①	90.07	75.98	75.73	73.51	71.41
②	2.083	2.700	2.721	2.882	3.045
③	2.084	2.700	2.720	2.881	3.043
④	112.3	111.4	111.3	110.1	109.2
⑤	112.3	111.4	111.2	110.1	109.2
⑥	1.970	1.956	1.956	1.957	1.960
⑦	1.562	1.557	1.557	1.557	1.557
⑧	1.970	1.956	1.956	1.957	1.960

Figure 5. B3LYP/LANL2DZ-optimized geometries (in Å and deg) of the cycloaddition products of $[(\text{SiH}_3)_2\text{Si}=\text{M}=\text{Si}(\text{SiH}_3)_2]^-$ (X = B, Al, Ga, In, and Tl). For the relative energies for each species see Table 1. Hydrogens are omitted for clarity.

in the central position and the most electronegative atom (such as Si) in the terminal position. Consequently, the previous theoretical predictions based on Su's work are in agreement with recent experimental observations.⁴

(2) The Geometries and Energetics of $[(\text{SiH}_3)_2\text{Si}=\text{M}=\text{Si}(\text{SiH}_3)_2]^-$ Cycloadditions. Next, let us consider mechanisms that proceed via eq 1, focusing on the transition states as well as on the [3 + 2] cycloaddition products themselves. Namely, the cycloaddition mechanisms may be thought to proceed as follows: reactants (12-valence-electron allenic anion species + C_2H_4) → transition state (TS) → cycloaddition products (Pro). The optimized geometries for these TS's and Pro's were calculated at the B3LYP/LANL2DZ level of theory, and their selected geometrical parameters are collected in Figures 4 and 5, respectively. The corresponding relative energies at the B3LYP and CCSD levels of theory are given in Table 1. The potential energy profiles based on the CCSD data in Table 1

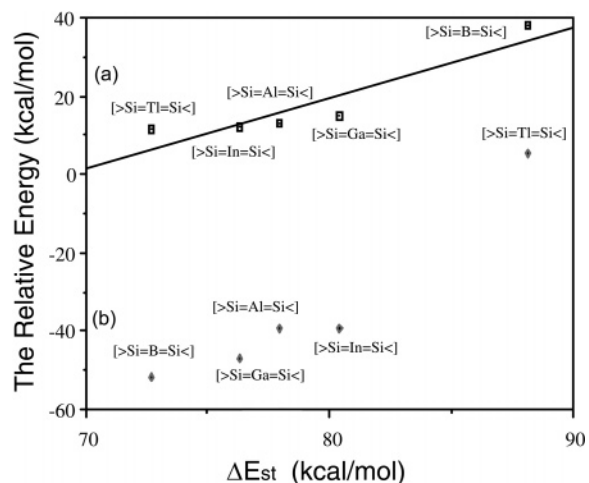


Figure 6. ΔE_{st} ($=E_{\text{triplet}} - E_{\text{singlet}}$) for $[(\text{SiH}_3)_2\text{Si}=\text{M}=\text{Si}(\text{SiH}_3)_2]^-$ vs the activation energy and reaction enthalpy for the cycloaddition of $[(\text{SiH}_3)_2\text{Si}=\text{M}=\text{Si}(\text{SiH}_3)_2]^-$ to ethylene. The linear regression equation is (a) $y = 1.798\Delta E_{\text{st}} - 124.3$ and (b) $y' = 3.766\Delta E_{\text{st}} - 332.3$ with a correlation coefficient $R = 0.84$ and $R = 0.92$, respectively. All values were calculated at the CCSD/LANL2DZ//B3LYP/LANL2DZ level. See the text.

are summarized in Figure 6. Cartesian coordinates are given in the Supporting Information. Several noteworthy features from Figures 4 and 5 and Table 1 are revealed.

The optimized transition states (**B-TS**, **Al-TS**, **Ga-TS**, **In-TS**, and **Tl-TS**) along with the calculated transition vectors are shown in Figure 4, respectively. The arrows in the figure indicate the directions in which the atoms move in the normal coordinate corresponding to the imaginary frequency. It is readily seen that these transition states connect the corresponding reactants to the cycloaddition products. Examination of the single imaginary frequency for each transition state ($378i \text{ cm}^{-1}$ for **B-TS**, $277i \text{ cm}^{-1}$ for **Al-TS**, $237i \text{ cm}^{-1}$ for **Ga-TS**, $194i \text{ cm}^{-1}$ for **In-TS**, and $109i \text{ cm}^{-1}$ for **Tl-TS**) provides an excellent confirmation of the concept of the cycloaddition process. Namely, the reactants approach each other with their molecular planes parallel and two new bonds are formed at the same time. These reactions appear to be concerted; we have been able to locate only one transition state for each reaction and have confirmed that it is a true transition state on the basis of frequency analysis.

A comparison of the five transition structures yields a number of trends. As can be seen in Figure 4, the primary similarity between these optimized transition states is a five-membered-ring-like structure of C_1 symmetry. Next, there is a dramatic effect on the intermolecular distances at the saddle points. Increasing the atomic weight of the central atom in the $[\text{>Si}=\text{M}=\text{Si}<]^-$ species causes a large increase in the Si–C distances. That is, the two newly forming bond lengths increase in the order **B-TS** (2.33 Å) < **Al-TS** (2.81 Å) < **Ga-TS** (2.89 Å) < **In-TS** (3.08 Å) < **Tl-TS** (3.56 Å) and **B-TS** (1.94 Å) < **Al-TS** (1.97 Å) \approx **Ga-TS** (1.97 Å) < **In-TS** (1.98 Å) < **Tl-TS** (1.99 Å). In addition, the present calculations indicate that the greater the atomic weight of the central atom M, the more asynchronous the [3 + 2] cycloaddition reaction. For instance, as already shown in Figure 4, in **B-TS**, **Al-TS**, **Ga-TS**, **In-TS**, and **Tl-TS** one of the stretching Si–M bonds is longer than the other.

Furthermore, it should be noted that the newly formed Si–C bonds in the transition structures are stretched by 18.3%, 43.5%, 47.8%, 57.2%, and 81.4% for **2-TS**, **3-TS**, **5-TS**, **4-TS**, and **1-TS**, respectively, relative to their final equilibrium values. Also, our B3LYP calculations suggest that the C=C double

bond is stretched by 11.0%, 9.89%, 10.4%, 9.09%, and 7.03% for **B-TS**, **Al-TS**, **Ga-TS**, **In-TS**, and **Tl-TS**, respectively, relative to its value in ethylene (1.331 Å). All these features strongly indicate that the transition structures for allenic anions with a more electronegative central atom take on a more product-like character than the allenic anions with a less electronegative central atom. Consequently, the barriers are encountered earlier in the cycloadditions of the latter than of the former. As will be shown below, this is consistent with the Hammond postulate,¹⁸ which associates an earlier transition state with a smaller barrier and a more exothermic reaction.

Besides this, it is readily seen that 12-valence-electron allenic anions containing a more electronegative central atom have a greater activation barrier to the [3 + 2] cycloaddition with ethylene. For instance, as demonstrated in Table 1 (CCSD calculations), since the electronegativity order is B (2.0) > Si (1.70) > Ga (1.60) > Al (1.50) = In (1.50) > Tl (1.40),¹⁸ the barrier height for the cycloaddition follows a similar trend. That is, the activation energy decreases in the order **B-TS** (38.3 kcal/mol) > **Ga-TS** (14.9 kcal/mol) > **Al-TS** (12.9 kcal/mol) > **In-TS** (12.2 kcal/mol) > **Tl-TS** (11.8 kcal/mol). This strongly indicates that the [3 + 2] cycloaddition with [$>Si=Al=Si<$]⁻, [$>Si=Ga=Si<$]⁻, [$>Si=In=Si<$]⁻, and [$>Si=Tl=Si<$]⁻ should take place more readily than with [$>Si=B=Si<$]⁻.

In summary, it is clear from the above barrier heights that the [3+2] cycloaddition reaction of 12-valence-electron allenic anions with ethylene occurs more readily if the most electronegative atoms are in the terminal rather than the central position.

The optimized product geometries (**B-Pro**, **Al-Pro**, **Ga-Pro**, **In-Pro**, and **Tl-Pro**) are collected in Figure 5. It is found that the newly formed Si–C bond in the transition structures are stretched by 0.575%, 0.613%, 0.613%, 0.920%, and 1.43% relative to their final equilibrium values in **B-Pro**, **Al-Pro**, **Ga-Pro**, **In-Pro**, and **Tl-Pro** cycloaddition products, respectively. Again, these features indicate that a 12-valence-electron allenic anion with a less electronegative atom in the central position reaches the transition state earlier than one with a more electronegative atom in the central position. Thus, one may anticipate a larger exothermicity for the former, which is confirmed by our CCSD calculations. For instance, the order of reaction enthalpies follows the same trend as the activation energy: **B-Pro** (+5.29 kcal/mol) > **Al-Pro** (–39.1 kcal/mol) > **Ga-Pro** (–39.2 kcal/mol) > **In-Pro** (–47.1 kcal/mol) > **Tl-Pro** (–51.8 kcal/mol). Note that **Al-Pro**, **Ga-Pro**, **In-Pro**, and **Tl-Pro** cycloaddition products are more exothermic than **B-Pro**. Thus, considering both the kinetics and the thermodynamics of the [3 + 2] cycloaddition reactions, one may conclude that cycloaddition of 12-valence-electron allenic anions (i.e., [$>Si=M=Si<$]⁻) with ethylene should produce a five-membered-ring cycloadduct compound in a single step (i.e., in a concerted manner), thus stereospecifically. In other words, such cycloaddition reactions should be favored for producing stereoretention products.

IV. Overview of [3 + 2] Cycloaddition Reaction

Taking all five 12-valence-electron allenic anions (i.e., [$>Si=M=Si<$]⁻) systems studied in this paper together, one can draw the following conclusions.

(1) The [3 + 2] cycloadduct resulting from the reaction of a 12-valence-electron allenic anion and an olefin should be formed in a one-step process. Namely, these [3 + 2] cycloadditions

proceed stereospecifically, leading to cycloproducts with retained stereochemistry.

(2) Regardless of the relative electronegativity of the central atom of the 12-valence-electron allenic anion, its cycloaddition reaction with ethylene is predicted to be concerted, but via an asynchronous transition state.

(3) A knowledge of the singlet–triplet splitting of the 12-valence-electron allenic anion is of great importance in understanding its reactivity since it can affect the driving force for cycloadditions.

(4) In principle, the more electronegative and the lighter the central atom in the 12-valence-electron allenic anion, the larger its ΔE_{st} , the higher the activation barrier, and the smaller the enthalpy of its cycloaddition to an alkene.

(5) Electronic as well as steric factors should play an important role in determining the chemical reactivity of the 12-valence-electron allenic anion species from both kinetic and thermodynamic viewpoints.

V. Origin of the Barrier Height and the Reaction Enthalpy for [(SiH₃)₂Si=M=Si(SiH₃)₂]⁻ Cycloadditions

In this section, an intriguing model for interpreting the relative reactivity of the reactants is provided by the so-called configuration mixing (CM) model, which is based on the work of Pross and Shaik.^{20,21} According to the conclusions of this model, the energy barriers governing processes as well as the reaction enthalpies should be proportional to the energy gaps for both [(SiH₃)₂Si=M=Si(SiH₃)₂]⁻ and ethylene, that is, ΔE_{st} ($=E_{\text{triplet}} - E_{\text{singlet}}$ for [(SiH₃)₂Si=M=Si(SiH₃)₂]⁻) + $\Delta E_{\pi\pi^*}$ ($=E_{\text{triplet}} - E_{\text{singlet}}$ for C₂H₄). For the CCSD calculations on the aforementioned five systems, a plot of activation barrier versus ΔE_{st} is given in Figure 6: $y = 1.798x - 124.3$ ($x = \Delta E_{st}$, $y =$ the activation energy). Likewise, a linear correlation between ΔE_{st} and the reaction enthalpy (y') is also obtained at the same level of theory: $y' = 3.766x - 332.3$. This investigation makes it quite evident that, in order to find a good model for the facile cycloaddition of 12-valence-electron allenic anion with ethylene, an understanding of its singlet–triplet splitting ΔE_{st} is crucial. We thus conclude that both the order of the singlet and triplet states and their energy separation are responsible for the existence and the height of the energy barrier.^{20,21}

Bearing these analyses in mind, we shall now explain the origin of the following observed trends: *Why does the reactivity of 12-valence-electron allenic anions increase in the order [$>Si=B=Si<$]⁻ < [$>Si=Al=Si<$]⁻ \approx [$>Si=Ga=Si<$]⁻ \approx [$>Si=In=Si<$]⁻ < [$>Si=Tl=Si<$]⁻?*

The reason for this can be traced to the singlet–triplet energy gap of the 12-valence-electron allenic anion ($[>Si=M=Si<]$, M = group 13 elements). That is to say, the smaller the ΔE_{st} for [(SiH₃)₂Si=M=Si(SiH₃)₂]⁻, the lower the barrier height and the larger the exothermicity and, in turn, the faster the cycloaddition reaction. As one can see in Figure 3, the HOMO–LUMO energy difference (and hence also ΔE_{st}) for a 12-valence-electron allenic anion (i.e., [(SiH₃)₂Si=M=Si(SiH₃)₂]⁻ in the

(19) Allred, A. L. *J. Inorg. Nucl. Chem.* **1961**, *17*, 215, and references therein.

(20) For details, see: (a) Shaik, S.; Schlegel, H. B.; Wolfe, S. In *Theoretical Aspects of Physical Organic Chemistry*; John Wiley & Sons Inc.: New York, 1992. (b) Pross, A. In *Theoretical and Physical Principles of Organic Reactivity*; John Wiley & Sons Inc.: New York, 1995. (c) Shaik, S. *Prog. Phys. Org. Chem.* **1985**, *15*, 197.

(21) (a) The first paper that originated the CM model: Shaik, S. *J. Am. Chem. Soc.* **1981**, *103*, 3692. (b) About the most updated review of the CM model: Shaik, S.; Shurki, A. *Angew. Chem., Int. Ed.* **1999**, *38*, 586.

(18) Hammond, G. S. *J. Am. Chem. Soc.* **1954**, *77*, 334.

present work) decreases rapidly from $M = \text{boron}$ down to thallium. Indeed, as can be seen in Table 1, our CCSD results suggest a decreasing trend in ΔE_{st} of $[(\text{SiH}_3)_2\text{Si}=\text{M}=\text{Si}(\text{SiH}_3)_2]^-$ of $[>\text{Si}=\text{B}=\text{Si}<]$ (88 kcal/mol) $>$ $[>\text{Si}=\text{Ga}=\text{Si}<]$ (80 kcal/mol) $>$ $[>\text{Si}=\text{Al}=\text{Si}<]$ (78 kcal/mol) $>$ $[>\text{Si}=\text{In}=\text{Si}<]$ (76 kcal/mol) $>$ $[>\text{Si}=\text{Tl}=\text{Si}<]$ (73 kcal/mol). This correlates well with the trend in both barrier height and exothermicity, as demonstrated in the previous section.

V. Conclusion

The present theoretical investigations present the first theoretical evidence that the chemical reactivity of 12-valence-electron allenic anion species increases in the order $[>\text{Si}=\text{B}=\text{Si}<]^- < [>\text{Si}=\text{Al}=\text{Si}<]^- \approx [>\text{Si}=\text{Ga}=\text{Si}<]^- \approx [>\text{Si}=\text{In}=\text{Si}<]^- < [>\text{Si}=\text{Tl}=\text{Si}<]^-$.

Besides this, our study has shown that the singlet–triplet gap $\Delta E_{\text{st}} (=E_{\text{triplet}} - E_{\text{singlet}})$ based on the CM model can provide a useful basis for understanding and rationalizing the relative magnitudes of the activation barriers as well as the reaction enthalpies for the cycloaddition reaction of 12-valence-electron allenic anion species with an alkene. We are confident in predicting that for the above 12-valence-electron allenic anion

systems a less electronegative as well as a heavier main group atom center will lead to a smaller ΔE_{st} and, in turn, will facilitate the cycloaddition reactions to alkene. Despite the fact that the estimated magnitude of the barrier and the predicted geometry of the transition state for such reactions appear to be dependent on the calculational level applied, our qualitative predictions are consistent with the computational results presented here. The predictions may be useful as a guide to future synthetic efforts and to indicate problems that merit further study by both theory and experiment.

It is ultimately hoped that this study will be helpful for further developments in group 13 chemistry.

Acknowledgment. We are grateful to the National Center for High-Performance Computing of Taiwan for generous amounts of computing time. We also thank the National Science Council of Taiwan for their financial support.

Supporting Information Available: Cartesian coordinates. This material is available free of charge via the Internet at <http://pubs.acs.org>.

OM7002943